Article

# Detection of CTCs in breast cancer patients by nanopore sensing with aptamer-mediated amplification

Xinqiong Li, Peng Zhang, Linqin Dou, Yu Wang, Ke Sun, Xialin Zhang, Guiqin Song, Changjian Zhao, Kaiju Li, Yunjin Bai, Xiaojun Zeng, Cuisong Zhou, Binwu Ying, Jie Chen, and Jia Geng

*ACS Sens.*, **Just Accepted Manuscript** • DOI: 10.1021/acssensors.9b02537 • Publication Date (Web): 11 May 2020

# Detection of CTCs in breast cancer patients by nanopore sensing with aptamer-mediated amplification

**Xinqiong Li[1#], Peng Zhang[1, 2#], Linqin Dou[1], Yu Wang[1], Ke Sun[1], Xialin Zhang[1], Guiqin Song[1], Changjian Zhao[1], Kaiju Li[1], Yunjin Bai[3], Xiaojun Zeng[1], Cuisong Zhou[4], Binwu Ying[1]*, Jie Chen[5]*, Jia Geng[1]***

[1] Department of Laboratory Medicine, State Key Laboratory of Biotherapy and Cancer Center, West China Hospital, Sichuan University and Collaborative Innovation Center, Chengdu 610041 China

[2] School of Pharmaceutical Sciences, Guangzhou Higher Education Mega Center, Sun Yat-sen University, Guangzhou 510006, China

[3] Department of Urology, West China Hospital, Sichuan University, Chengdu 610041, China

[4] College of Chemistry, Sichuan University, Chengdu 610041, China

[5] Department of Breast Surgery, Clinical Research Center for Breast, West China Hospital, Sichuan University, Chengdu 610041, China

**Corresponding Author:** geng.jia@scu.edu.cn **(**J.G), chenjiedoctor@126.com (J.C.), docybw @gmail.com (B.W.Y.)

[#] These authors contributed equally to this work.

**Abstract**

Circulating tumor cells (CTCs) has been utilized in the diagnosis and prognosis of tumor. However, the CTC concentration is extremely low to be detected in peripheral blood. Many existing methods suffer from either expensive labeling or complex operation. In this study, we constructed a label- and enzyme-free and sensitive method to detect the breast cancer CTCs. First of all, a probe containing a breast cancer cell-specific aptamer and a complementary single-stranded DNA (trigger DNA P1) were designed. When the target cells are present, the aptamer binds to the CTCs and releases P1 which trigger the strand displacement amplification (SDA). This process generates three-way junction (3WJ) structure DNA, the specific translocation signals of which are identified by nanopore assay. The detection limit of tumor cells is 5 in the current experiment setup, and can be further reduced. Furthermore, the method is demonstrated in clinical samples test with high recovery rate and accuracy. Our results suggest that this method could be applied to early diagnosis

of metastatic recurrence and prognosis determination.

***Keywords:*** Circulating tumor cell, aptamer-assisted amplification, nanopore, biosensor, breast cancer

Breast cancer is a leading cause of death among women worldwide, with an estimated mortality of 626, 279 every year [1]. In the USA, the incidence of breast cancer in 2015 is 271,270 and the mortality is 42, 260 [2]. While in China, low income and lack in health care facilities have triggered a higher morbidity[3]. Early diagnosis has a great significance in the therapy of breast cancers, and is a key factor in increasing survival rate. The current gold standard of breast cancer diagnosis is the histological examination of tumor tissue; however, this method is invasive and risky for patients. In recent years, non-invasive methods used to detect the tumor-relative biomarkers in blood gain increasing attention in the oncology community. Circulating tumor cells (CTCs) detached from primer tumors penetrate into peripheral blood, providing rich heterogeneity information of DNA, RNA and proteins about different patients. Detecting the types and the amounts of CTCs enables real-time monitoring the dynamic of tumors. Therefore, for early diagnosis and prognosis analysis of cancers, CTCs have been investigated to obtain abundant information facilitating the monitoring and treatment of tumor. Studies on both advanced breast cancer and early breast cancer have demonstrated that the CTCs are clinically efficient for tumor diagnosis [4–6]. The CTCs in peripheral blood are rare, which are often undetectable by regular high-resolution imaging technologies. Various methods for CTCs assay have been developed, including polymerase chain reaction (PCR), cytometric methods and immunohistochemistry, etc., but high cost and long detection time limit their applications in clinical diagnosis [7]. Therefore, there is still an urgent need to develop a new method of high accuracy, ultra-sensitivity, highly-efficiency and low-cost for the detection of breast cancer.

Aptamers are oligonucleotides or peptides with a strong binding affinity to target molecules. They are generated via Systematic Evolution of Ligands by Exponential enrichment (SELEX) *in vitro* [8]. Aptamers are widely utilized to detect various cancer cells because it has many advantages over antibody probes, including convenient synthesis, high binding affinity and specificity, good stability and low variability between different batches [9–15]. Epithelial mucin-1 (MUC-1) is a membrane

glycoprotein overexpressed in 90% of breast cancer, which can act as an effective marker for breast cancer CTCs [16]. However, only a few label-free and enzyme-free aptamer-based biosensors detecting cancer cells have been reported [17,18].

Target-induced strand displacement amplification (T-SDA) is a kind of isothermal reaction. One strand of the double-stranded DNA or one toehold of the hairpin DNA is replaced by the trigger DNA strand in the overhanging single-stranded domain, generating a DNA duplex with higher thermodynamic and kinetic stability [19]. T-SDA has gained increasing attention, particularly in fluorescent detection [19,20], whereas the reported T-SDAs need to be meliorate because the number of trigger sequences recycling is limited. Biological nanopores sensing of biomolecules at the single-molecule sensitivity level have shown vast potential in the label-free and real-time detection of DNA, RNA and proteins [21–24]. Herein, a simple and sensitive method for the detection of breast cancer cells is developed based on aptamer recognition, target-induced hairpin assembly-assisted amplification, and detection by nanopore *Mycobacterium smegmatis* porin A (MspA). First of all, the breast cancer cell line MCF-7 overexpressing MUC-1 on the cell surface is selected as CTC model, and a probe containing a MUC-1 specific aptamer and its partially complementary single-stranded DNA P1 is designed [25]. When the target cells are present, the aptamer binds to the target protein on the cell. At the same time, P1 is released to trigger the SDA, followed by the formation of 3WJ structure DNA which generates specific signals that is detectable by nanopore. The usage of trigger DNA P1 achieves cascade amplification of cancer cells. With the participation of aptamer recognition and cascade amplification, this assay show excellent sensitivity and high specificity for breast cancer cells detection, and could be used for clinical diagnosis of CTCs. Various other methods could be used for the assay of 3WJ DNA in additional to nanopore assay with their own advantages, for example the highly sensitive and real-time observation by FRET. For clinical diagnostics, especially POCT, nanopore devices could be suitable due to its sensitivity, portability (size of a smart phone), and real-time rapid assay.

## Results and Discussion

### Principle of the design

The principle of aptamer-mediated SDA detecting MCF-7 cells was descried in **Figure 1**. The strategy mainly consisted of three parts: ( i ) cell-specific aptamer was bound to the target cell to

release trigger DNA P1; ( ⅱ ) the SDA was triggered by P1, generating 3WJ DNA; ( ⅲ ) 3WJ DNA was then detected by MspA nanopore. The aptamer was partially complementary to P1 to avoid nonspecific amplification. When the target cells were present, the aptamer (domain colored in purple) bound to the cell and P1 was released. Then the 5' of P1 strand complementarily bound to the overhang of HA, opening up the hairpin structure. The exposed segment of HA bound to HB, opening HB subsequently. The exposed segment of HB bound to HC, and displaced the P1 to form the 3WJ structure while P1 triggered the next cycle in succession. The resulting 3WJ structure were detected with MspA nanopore.

**Confirmation of 3WJ structure with Native PAGE and MspA nanopore**

Native PAGE was used to confirm the SDA performance in the formation of 3WJ structure. As shown in **Figure S1b**, two bands were obtained in lane 5, corresponding to HA, HB (upper band) and HC (lower band). Three bands were observed in lane 8, and two bands were obtained compared with lane 5. The **Figure S1b** also showed that the location of 3WJ structure was different from P1-HA and P1-HA-HB. The monomer P1 (lane 4) migrated slower than monomer HC (lane 1), indicating that the mobility of P1-HA-HB was lower than 3WJ. Those data suggested that SDA reaction couldn't be triggered and the 3WJ structure couldn't be formed without P1. The formation of 3WJ was further verified by atomic force microscopy (AFM) (Figure S1c).

Before detecting the cells, we first characterized the signals of the 3WJ structure translocating through MspA nanopore. In this study, a mixture of HA, HB and HC was set as control (HA-HB-HC), while mixture of HA, HB, HC and P1 was set as experiment group (P1-HA-HB-HC), in which P1was able to trigger the formation of 3WJ. The purified 3WJ structure was set as positive control. In this report, open current was defined as $I_o$, blockage current caused by analytes translocating through the pore was $I$, and the blockage ratio was $I/I_o$. Scatter plot in **Figure 2** and **Figure S2** showed that there were two current blockages in both groups, in which the group with small blockage was labeled as E1 and the group with deep blockage was labeled as E2. Data analysis indicated that the blockage ratios of E1 and E2 were $0.37 \pm 0.01$ and $0.85 \pm 0.01$ (Gauss distribution fitting), respectively. Since the blockage ratio of low blockage signals was much lower than ssDNA strand translocating through MspA nanopore, we proposed that they were generated by the hairpin DNA rattles in the vestibule [26]. Along with the applied voltage increasing from 80 to 120 mV,

experiment showed that the blockage of E1 increased gradually (**Figure S3**), which was consistent with previous report [27]. The high blockage signals (E2) corresponded to ssDNA translocating through MspA nanopore. The dwell time of E1 in HA-HB-HC and P1-HA-HB-HC were 2.08 ± 0.04 ms and 1.93 ± 0.04 ms, respectively. The histogram of P1-HA-HB-HC unzipping time showed two peaks at 0.73 ± 0.04 ms and 3.12± 0.01 ms, respectively (**Figure S2c**). The former value was similar to that of HA-HB-HC at 0.5± 0.03 ms. This indicated that the blockage events with short dwell time are caused by hairpin DNA, while the blockage events with long dwell time were caused by 3WJ structure. Further study showed that the unzipping of E2 was dependent on the voltage (**Figure S4**). Combing the blockage and dwell time analysis, we concluded that the events with deep blockage (≥0.8) and long unzipping time (≥100 ms) were generated by 3WJ unzipping and translocating through MspA nanopore. To monitor MCF-7 cells, those events with similar blockage and unzipping time for the target signal were also observed. This result suggested that aptamer could bind to MCF-7 cells and P1 was released to trigger SDA reaction.

**Optimization of the nanopore assay**

To increase the sensitivity of the nanopore assay, the incubation time and the concentration of P1: HA/HB/HC DNA for the formation of 3WJ were optimized. Optimal reaction time and DNA concentration were investigated by comparing the frequency of the target events using nanopore assay. As shown in **Figure S5a**, the frequency of 3WJ translocation increased as the concentration of HA/HB/HC increased from 5 nM to 15 nM, but decreased with higher concentration. Figure S4b showed that with the increasing of reaction time, the translocation frequency also increased and reached a stable level at 3 h. As a result, 3 h was chosen as the reaction time, and the concentration of P1: HA/HB/HC was set as 1 nM : 15 nM in the following experiment.

**Specificity and sensitivity of nanopore assay**

To evaluate the sensitivity of nanopore assay, we tested different numbers of MCF-7, ranging from 5 to 1000, in the detecting system. As shown in **Figure 3**, no signature events of 3WJ translocation were detected in the absence of MCF-7 cells. As cell number increased, the events frequency increased gradually. There was a good linear relationship between the frequency of signals and the logarithm of cell number in the range of 5 to 1000, with $R^2$ value of 0.9958. Longer current trace

recording of 4 min were provided in **Figure S6**. It is interesting to see that as the number of cells increase, the slope of events frequency vs. number of cells decrease. This phenomenon could be explained by the saturation of high blockage events brought by 3WJ. As we can see from **Figure 3c**, the high blockage events for 50 and 100 cells occupied remarkable percentage of entire trace section. We can deduce that with the continuous increase of cell number above 100, the increase of the number of specific events slows down. The limit of detection was 5 cells in this report, which showed comparable or higher sensitivity in the detection of mammary cancer cells [18,28–33]. The high sensitivity of nanopore test may benefit from the high affinity of aptamer and multiple cycle amplification. Therefore, this assay could be used for detecting low number of cells, such as CTCs. To evaluate the specificity of this sensing strategy, HepG2 and U-87MG cells without overexpression of MUC-1 biomarkers were used as control cells. The final number of cells used in this experiment was 100. No signature events were observed in absence of target cells. As shown in **Figure 4**, the frequency of signals of HepG2 and U-87MG were as low as the blank group, while the MCF-7 cells group showed significant higher frequency, on account of the high specific binding ability of aptamer to the target cells. The stability of the hairpins also played a significant role in high specificity of the biosensors.

**Detection of clinical samples**

We collected the peripheral blood samples from 3 healthy women, and 7 patients diagnosed and treated for breast cancer at the Department of Breast Surgery, West China Hospital of Sichuan University, to further confirm the clinical effectiveness. MCF-7 cells from human peripheral blood samples were detected by our developed strategy. Different amounts of MCF-7 cells were added into the blood samples from 3 healthy women. As shown in **Table 1**, the recovery rate of MCF-7 cells was up to 85%. Furthermore, the blood of 7 patients were assayed. CTCs were collected according to the manufacture's instruction of the CELLection Epithelial Enrich Dynabeads and incubated with aptamer-P1 and HA/HB/HC. The mixtures were detected by nanopore assay, and the events with deep blockage ($\geqslant$0.8) and long unzipping time ($\geqslant$100 ms) were acquired. Analysis of the results from patients' blood samples show a frequency of events ranged from 0.9 to 3.1 $min^{-1}$ (**Figure 5**), and number of CTCs ranging from 5 to 135 (1.25 to 22.5 $mL^{-1}$). Those results were consistent with their medical imaging diagnosis (**Table 2**). Comparing to healthy people, these

patients showed more CTCs in their blood.

These results indicated that this method could be used in clinical samples detection, with a high potential in practical applications. It took no more than 5 h to detect the CTCs from blood using the developed nanopore assay. Compared with CellSearch, PCR and other methods (**Table S2**), this method was label-free, less time-consuming [33], low-cost and easy-operation. MUC-1 is over-expressed in 90% of mammary cancer cells, and MUC-1 can be expressed in many epithelial tumor cells, such as renal cancer A549 cell, colon cancer HT-29 cell, mammary cancer ZR-75-1 cell, mammary cancer BT-20 cell, mammary cancer T47D cell, pancreatic cancer PANC-1 cell, pancreatic cancer BxPC3 cell, ovarian cancer OVCAR-3 cell and bladder cancer MGHu3 cell. This indeed could generate false positive signals. In the clinical setting, the false positive could be eliminated in combination with other clinical diagnosis. For certain applications, such as prognosis during or after treatment of breast cancer patients, periodical inspection of CTC including nanopore assay method could be an effective tool for monitoring of recrudesce.

## Conclusion

In summary, a simple, label-free, enzyme-free, highly-efficient and sensitive method for cancer cells detection is developed in this study. Benefiting from aptamer recognition, SDA reaction and the specific translocation signals of 3WJ through MspA nanopore, this method achieves an ultra-sensitive detection of 5 breast cancer cells. The detection limit of was 5 CTCs in 4 mL blood samples from commercially available electrophysiological measurement chamber of 1 mL volume. If a customized chamber of 0.1 mL is used, the detection sensitivity/cutoff value could reach $\geqslant$1 CTC, which will be comparable to the best current methods. Furthermore, it shows high detection accuracy, rapid test for clinic samples comparing to other traditional analysis approaches, with great potential in early diagnosis of metastatic recurrence and determination of prognosis.

Moreover, the principle of developed biosensor could be extended to detect other tumor CTCs, such as lung and liver cancer, as well as other disease related targets by designing corresponding aptamers. There are some well-developed technologies, including microfluidics, etc., that enables automated extraction of CTCs from blood samples. We may combine the advantages of both systems of extraction by microfluidics and detection by nanopore, or event integrate them in future studies.

## Experimental Section

### Materials

The oligonucleotides (HPLC purified) were synthesized by Sangon Biotech Co., Ltd. (Shanghai, China) and the sequences are listed in **Table S1**. Sodium ascorbate and 3-(N-morpholino) propanesulfonic acid (MOPS) and Decane (anhydrous, ≥95%) were obtained from Sigma-Aldrich Sigma-Aldrich Co., Ltd. (St. Louis, MO, USA). CELLection Epithelial Enrich Dynabeads was purchased from Invitrogen (California, U.S.A.). Dulbecc's modified Eagle's medium (DMEM), Minimum Essential Media (MEM), Trypsin-EDTA, and 1×phosphate buffered saline (PBS) were obtained from Gibco (California, U.S.A). Fetal bovine serum (FBS) and penicillin-streptomycin were obtained from Hyclone (Logan, UT, USA). 1, 2-Diphytanoyl-sn-glycero-3-phosphocholine was obtained from Avanti Polar Lipids Inc. (Alabaster, AL, USA). The other chemicals were of analytical grade and ultrapure water (18.2 MΩ/cm) was used.

### Cell culture and preparation

Breast cancer MCF-7 cells, human hepatoma HepG2 cells and human glioblastoma U-87 MG cells were purchased from Cell Bank of the Typical Culture Preservation Committee, Chinese Academy of Sciences (Shanghai, China). MCF-7, HepG2 and U-87 MG were cultured in MEM with 10% FBS and 1% penicillin-streptomycin, maintained at 37 °C in an atmosphere with 5% $CO_2$. All the cells were collected in the logarithmic phase and digested with trypsin, washed twice with PBS, centrifuged at 600 ×*g* for 5 min, then suspended by adding 1×PBS. Cell density was calculated by using Countstar BioTech Automated Cell Counter (Shanghai, China). In order to obtain the minimum cell number, cells were diluted with 1×PBS. Finally, 1 uL cell suspension was placed in the culture dish for cell counting to ensure that the minimum number of cells could be observed.

### DNA preparation and catalytic hairpin assembly

All the oligonucleotides were diluted with double distilled water ($ddH_2O$) to 100 uM. 10 uM aptamer and 10 uM P1 were incubated at 95°C for 5min, then gradually cooled down to RT. 50 nM aptamer-P1 complex and the cell suspension were mixed with MOPS buffer (10 mM MOPS, 150 mM NaCl, 2 mM $MgCl_2$, pH 7.4) to 100 uL. The mixture was incubated in PCR system (Applied Biosystems, Inc, USA) at 37°C for 1 h and centrifuged at 600 ×*g* for 5 min, and the supernatant was

obtained and used to trigger the SDA. Hairpin A (HA), hairpin B (HB) and hairpin C (HC) were annealed separately at 95°C for 5 min, then gradually cooled to RT. The abovementioned supernatant was mixed with 750 nM HA/HB and HC, and reacted in PCR system at 37°C for 3 h. Those products were analyzed by 15% native polyacrylamide gel electrophoresis (PAGE) in 1×TBE buffer (89 mM Tris-boric, 2 mM EDTA, pH 8.0) and visualized under UV light using Gel Doc EZ System (Bio-Rad, USA). The 3WJ was purified using TIANgel purification kit (TIANGEN Biotech Co., Ltd. Beijing, China). The products of P1-HA-HB-HC were also analyzed by AFM. The samples were diluting with $ddH_2O$ containing 1 mM $Mg^{2+}$ and then dropped onto a fresh cleaved mica surface. After adsorption for 20 min, the mica was lightly rinsed by $ddH_2O$ and dried with pure nitrogen. AFM results were obtained using MultiMode 8 nanoscope under ScanAsyst Mode with a scanasyst-air tip (Bruker, Germany).

**Collection of clinical samples**

This study was approved by the Biomedical Ethics Committee of West China Hospital, Sichuan University (2019-326). Patients were diagnosed and treated for breast cancer at the Department of Breast Surgery, West China Hospital of Sichuan University. The peripheral blood samples were collected in operation room. Samples from healthy people (n=3) as well as breast cancer patients (n=7) were collected into K2 EDTA blood tube and stored at room temperature for further experiment.

To remove the complex matrix in clinical samples, the blood samples were treated using CELLection Epithelial Enrich Dynabeads according to the manufacturer's instructions to enrich the CTCs (Please see Methods in Supplementary Information). The released cells were collected and washed twice with PBS, followed by centrifugation at 600 × *g* for 5 min and resuspension with MOPS. The following steps of CTC enrichment were conducted in the same way with that for MCF-7 as described above for nanopore assay.

**Nanopore test and data analysis**

The phospholipid bilayer was formed with 1, 2-Diphytanoyl-sn-glycero-3-phosphocholine across a 150 μm aperture in a Delrin bilayer cup (Warner Instruments, Hamden, CT). 1 mL conducting buffer were added to both sides of the chambers (*cis*: 0.5 M NaCl, 10 mM Tris-HCl, pH 8.0); *trans*: 3 M

NaCl, 10 mM Tris-HCl, pH 8.0). Both MspA nanopore solution and DNA molecule were added to the *cis* side.

The ionic current was measured using patch clamp device EPC 10 *USB* 10.6 (Heka Electronic, Darmstadt, Germany) and filtered using a lowpass Bessel filter of 10 kHz at a sampling rate of 50 kHz. Clampfit 10.6 (Molecular Devices), Excel (Microsoft, Redmond, WA, USA) and OriginLab 9.0 (OriginLab Corporation, Northampton, MA, USA) were used for data analysis. All the experiments were conducted at RT 22 ± 2 °C.

**ASSOCIATED CONTENT**

**Supporting information available:**

DNA sequences employed in this work; Scatter plot and histograms showing blockades and unzipping time by hairpin and 3WJ; Voltage dependence of the nanopore events; Experimental conditions; Current traces from clinic samples.

**Author Contributions**

[#] These authors contributed equally to this work.

## Acknowledgments

This work was supported by the National Key Research and Development Program of China (2016YFA0201400 and 2016YFC1200300), and National Natural Science Foundation of China (81574038).

## Conflict of interest

The authors declare no conflict of interest.

## References

(1) Bray, F.; Ferlay, J.; Soerjomataram, I.; Siegel, R. L.; Torre, L. A.; Jemal, A. Global Cancer Statistics 2018: GLOBOCAN Estimates of Incidence and Mortality Worldwide for 36 Cancers in 185 Countries. *CA Cancer J Clin* **2018**, *68* (6), 394–424. https://doi.org/10.3322/caac.21492.

(2) Siegel, R. L.; Miller, K. D.; Jemal, A. Cancer Statistics, 2019 (US Statistics). *CA Cancer J Clin*

**2019**, *69* (1), 7–34. https://doi.org/10.3322/caac.21551.

(3) Azim, H. A.; Ibrahim, A. S. Breast Cancer in Egypt, China and Chinese: Statistics and Beyond. *Journal of Thoracic Disease*. 2014, pp 864–866. https://doi.org/10.3978/j.issn.2072-1439.2014.06.38.

(4) Lianidou, E. S.; Markou, A.; Strati, A. The Role of Ctcs as Tumor Biomarkers. In *Advances in Experimental Medicine and Biology*; 2015; Vol. 867, pp 341–367. https://doi.org/10.1007/978-94-017-7215-0_21.

(5) Bidard, F. C.; Peeters, D. J.; Fehm, T.; Nolé, F.; Gisbert-Criado, R.; Mavroudis, D.; Grisanti, S.; Generali, D.; Garcia-Saenz, J. A.; Stebbing, J.; et al. Clinical Validity of Circulating Tumour Cells in Patients with Metastatic Breast Cancer: A Pooled Analysis of Individual Patient Data. *Lancet Oncol* **2014**. https://doi.org/10.1016/S1470-2045(14)70069-5.

(6) Lucci, A.; Hall, C. S.; Lodhi, A. K.; Bhattacharyya, A.; Anderson, A. E.; Xiao, L.; Bedrosian, I.; Kuerer, H. M.; Krishnamurthy, S. Circulating Tumour Cells in Non-Metastatic Breast Cancer: A Prospective Study. *Lancet Oncol* **2012**, *13* (7), 688–695. https://doi.org/10.1016/S1470-2045(12)70209-7.

(7) Wang, J.; Dong, H. yan; Zhou, Y.; Han, L. yu; Zhang, T.; Lin, M.; Wang, C.; Xu, H.; Wu, Z. S.; Jia, L. Immunomagnetic Antibody plus Aptamer Pseudo-DNA Nanocatenane Followed by Rolling Circle Amplication for Highly-Sensitive CTC Detection. *Biosens Bioelectron* **2018**, *122*, 239–246. https://doi.org/10.1016/j.bios.2018.09.025.

(8) Jing, Z.; Pingang, H.; Yuzhi, F. Aptamer-Based Biosensor. *Prog Chem* **2009**, *21* (4), 732–738. https://doi.org/10.1016/j.trac.2007.12.004.

(9) Tan, W.; Donovan, M. J.; Jiang, J. Aptamers from Cell-Based Selection for Bioanalytical Applications. *Chem Rev* **2013**, *113* (4), 2842–2862. https://doi.org/10.1021/cr300468w.

(10) Zhang, P.; Liu, H.; Ma, S.; Men, S.; Li, Q.; Yang, X.; Wang, H.; Zhang, A. A Label-Free Ultrasensitive Fluorescence Detection of Viable Salmonella Enteritidis Using Enzyme-Induced Cascade Two-Stage Toehold Strand-Displacement-Driven Assembly of G-Quadruplex DNA. *Biosens Bioelectron* **2016**. https://doi.org/10.1016/j.bios.2016.02.031.

(11) Zhang, P.; Liu, H.; Li, X.; Ma, S.; Men, S.; Wei, H.; Cui, J.; Wang, H. A Label-Free Fluorescent Direct Detection of Live Salmonella Typhimurium Using Cascade Triple Trigger Sequences-Regenerated Strand Displacement Amplification and Hairpin Template-Generated-Scaffolded

Silver Nanoclusters. *Biosens Bioelectron* **2017**. https://doi.org/10.1016/j.bios.2016.09.037.

(12) Bi, S.; Ji, B.; Zhang, Z.; Zhang, S. A Chemiluminescence Imaging Array for the Detection of Cancer Cells by Dual-Aptamer Recognition and Bio-Bar-Code Nanoprobe-Based Rolling Circle Amplification. *Chem Commun* **2013**, *49* (33), 3452–3454. https://doi.org/10.1039/c3cc39296a.

(13) Jie, G.; Wang, L.; Yuan, J.; Zhang, S. Versatile Electrochemiluminescence Assays for Cancer Cells Based on Dendrimer/CdSe-ZnS-Quantum Dot Nanoclusters. *Anal Chem* **2011**, *83* (10), 3873–3880. https://doi.org/10.1021/ac200383z.

(14) Min, K.; Song, K. M.; Cho, M.; Chun, Y. S.; Shim, Y. B.; Ku, J. K.; Ban, C. Simultaneous Electrochemical Detection of Both PSMA (+) and PSMA (-) Prostate Cancer Cells Using an RNA/Peptide Dual-Aptamer Probe. *Chem Commun* **2010**, *46* (30), 5566–5568. https://doi.org/10.1039/c002524k.

(15) Wu, P.; Gao, Y.; Zhang, H.; Cai, C. Aptamer-Guided Silver-Gold Bimetallic Nanostructures with Highly Active Surface-Enhanced Raman Scattering for Specific Detection and near-Infrared Photothermal Therapy of Human Breast Cancer Cells. *Anal Chem* **2012**, *84* (18), 7692–7699. https://doi.org/10.1021/ac3015164.

(16) Rakha, E. A.; Boyce, R. W. G.; El-Rehim, D. A.; Kurien, T.; Green, A. R.; Paish, E. C.; Robertson, J. F. R.; Ellis, I. O. Expression of Mucins (MUC1, MUC2, MUC3, MUC4, MUC5AC and MUC6) and Their Prognostic Significance in Human Breast Cancer. *Mod Pathol* **2005**, *18* (10), 1295–1304. https://doi.org/10.1038/modpathol.3800445.

(17) Zhang, Y.; Chen, Z.; Tao, Y.; Wang, Z.; Ren, J.; Qu, X. Hybridization Chain Reaction Engineered DsDNA for Cu Metallization: An Enzyme-Free Platform for Amplified Detection of Cancer Cells and MicroRNAs. *Chem Commun* **2015**, *51* (57), 11496–11499. https://doi.org/10.1039/c5cc03144c.

(18) Chiu, W. J.; Ling, T. K.; Chiang, H. P.; Lin, H. J.; Huang, C. C. Monitoring Cluster Ions Derived from Aptamer-Modified Gold Nanofilms under Laser Desorption/Ionization for the Detection of Circulating Tumor Cells. *ACS Appl Mater Interfaces* **2015**, *7* (16), 8622–8630. https://doi.org/10.1021/acsami.5b00731.

(19) Zhang, J.; Li, C.; Zhi, X.; Ramón, G. A.; Liu, Y.; Zhang, C.; Pan, F.; Cui, D. Hairpin DNA-Templated Silver Nanoclusters as Novel Beacons in Strand Displacement Amplification for MicroRNA Detection. *Anal Chem* **2016**, *88* (2), 1294–1302.

https://doi.org/10.1021/acs.analchem.5b03729.

(20) Du, Y. C.; Jiang, H. X.; Huo, Y. F.; Han, G. M.; Kong, D. M. Optimization of Strand Displacement Amplification-Sensitized G-Quadruplex DNAzyme-Based Sensing System and Its Application in Activity Detection of Uracil-DNA Glycosylase. *Biosens Bioelectron* **2016**, *77*, 971–977. https://doi.org/10.1016/j.bios.2015.10.080.

(21) Howorka, S.; Cheley, S.; Bayley, H. Sequence-Specific Detection of Individual DNA Strands Using Engineered Nanopores. *Nat Biotechnol* **2001**. https://doi.org/10.1038/90236.

(22) Japrung, D.; Henricus, M.; Li, Q.; Maglia, G.; Bayley, H. Urea Facilitates the Translocation of Single-Stranded DNA and RNA through the α -Hemolysin Nanopore. *Biophys J* **2010**. https://doi.org/10.1016/j.bpj.2009.12.4333.

(23) Movileanu, L.; Howorka, S.; Braha, O.; Bay-ley, H. Detecting Protein Analytes That Modulate Transmembrane Movement of a Polymer Chain within a Single Protein Pore. *Nat Biotechnol* **2000**, *18* (10 SUPPL.), 1091–1095. https://doi.org/10.1038/80295.

(24) Cheley, S.; Xie, H.; Bayley, H. A Genetically Encoded Pore for the Stochastic Detection of a Protein Kinase. *ChemBioChem* **2006**, *7* (12), 1923–1927. https://doi.org/10.1002/cbic.200600274.

(25) Stecker, J. R.; Savage, A. A.; Bruno, J. G.; García, D. M.; Koke, J. R. Dynamics and Visualization of MCF7 Adenocarcinoma Cell Death by Aptamer-C1q-Mediated Membrane Attack. *Nucleic Acid Ther* **2012**, *22* (4), 275–282. https://doi.org/10.1089/nat.2012.0355.

(26) Vercoutere, W.; Winters-Hilt, S.; Olsen, H.; Deamer, D.; Haussler, D.; Akeson, M. Rapid Discrimination among Individual DNA Hairpin Molecules at Single-Nucleotide Resolution Using an Ion Channel. *Nat Biotechnol* **2001**. https://doi.org/10.1038/85696.

(27) Luan, B.; Zhou, R. Nanopore-Based Sensors for Detecting Toxicity of a Carbon Nanotube to Proteins. *J Phys Chem Lett* **2012**, *3* (17), 2337–2341. https://doi.org/10.1021/jz3007832.

(28) Xi, D.; Li, Z.; Liu, L.; Ai, S.; Zhang, S. Ultrasensitive Detection of Cancer Cells Combining Enzymatic Signal Amplification with an Aerolysin Nanopore. *Anal Chem* **2018**, *90* (1), 1029–1034. https://doi.org/10.1021/acs.analchem.7b04584.

(29) Cai, S.; Chen, M.; Liu, M.; He, W.; Liu, Z.; Wu, D.; Xia, Y.; Yang, H.; Chen, J. A Signal Amplification Electrochemical Aptasensor for the Detection of Breast Cancer Cell via Free-Running DNA Walker. *Biosens Bioelectron* **2016**. https://doi.org/10.1016/j.bios.2016.05.003.

(30) Qiu, Y.; Wen, Q.; Zhang, L.; Yang, P. Label-Free and Dynamic Evaluation of Cell-Surface Epidermal Growth Factor Receptor Expression via an Electrochemiluminescence Cytosensor. *Talanta* **2016**, *150*, 286–295. https://doi.org/10.1016/j.talanta.2015.12.019.

(31) Yang, Y.; Fu, Y.; Su, H.; Mao, L.; Chen, M. Sensitive Detection of MCF-7 Human Breast Cancer Cells by Using a Novel DNA-Labeled Sandwich Electrochemical Biosensor. *Biosens Bioelectron* **2018**, *122*, 175–182. https://doi.org/10.1016/j.bios.2018.09.062.

(32) Zhao, J.; Zhang, L.; Chen, C.; Jiang, J.; Yu, R. A Novel Sensing Platform Using Aptamer and RNA Polymerase-Based Amplification for Detection of Cancer Cells. *Anal Chim Acta* **2012**, *745*, 106–111. https://doi.org/10.1016/j.aca.2012.07.030.

(33) Wang, W.; Liu, S.; Li, C.; Wang, Y.; Yan, C. Dual-Target Recognition Sandwich Assay Based on Core-Shell Magnetic Mesoporous Silica Nanoparticles for Sensitive Detection of Breast Cancer Cells. *Talanta* **2018**, *182*, 306–313. https://doi.org/10.1016/j.talanta.2018.01.067.

## Figures and Tables

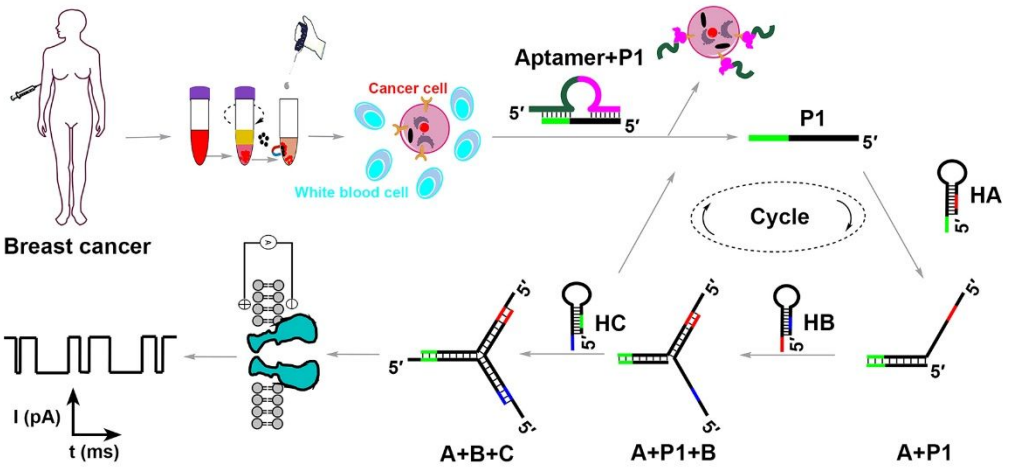


**Figure 1.** The scheme of detection of CTCs in serum from breast cancer patients using the nanopore sensor on the basis of aptamer-mediated amplification. CTCs cells are separated from patient's serum using magnetic beads. A specific cancer CTCs targeting aptamer is complementary with a single strand DNA P1. In the presence of target CTCs cells, P1 can be released to trigger the formation of 3WJ, which can be amplified with the circulation of P1, and then be detected using nanopore system by generating specific current signals.

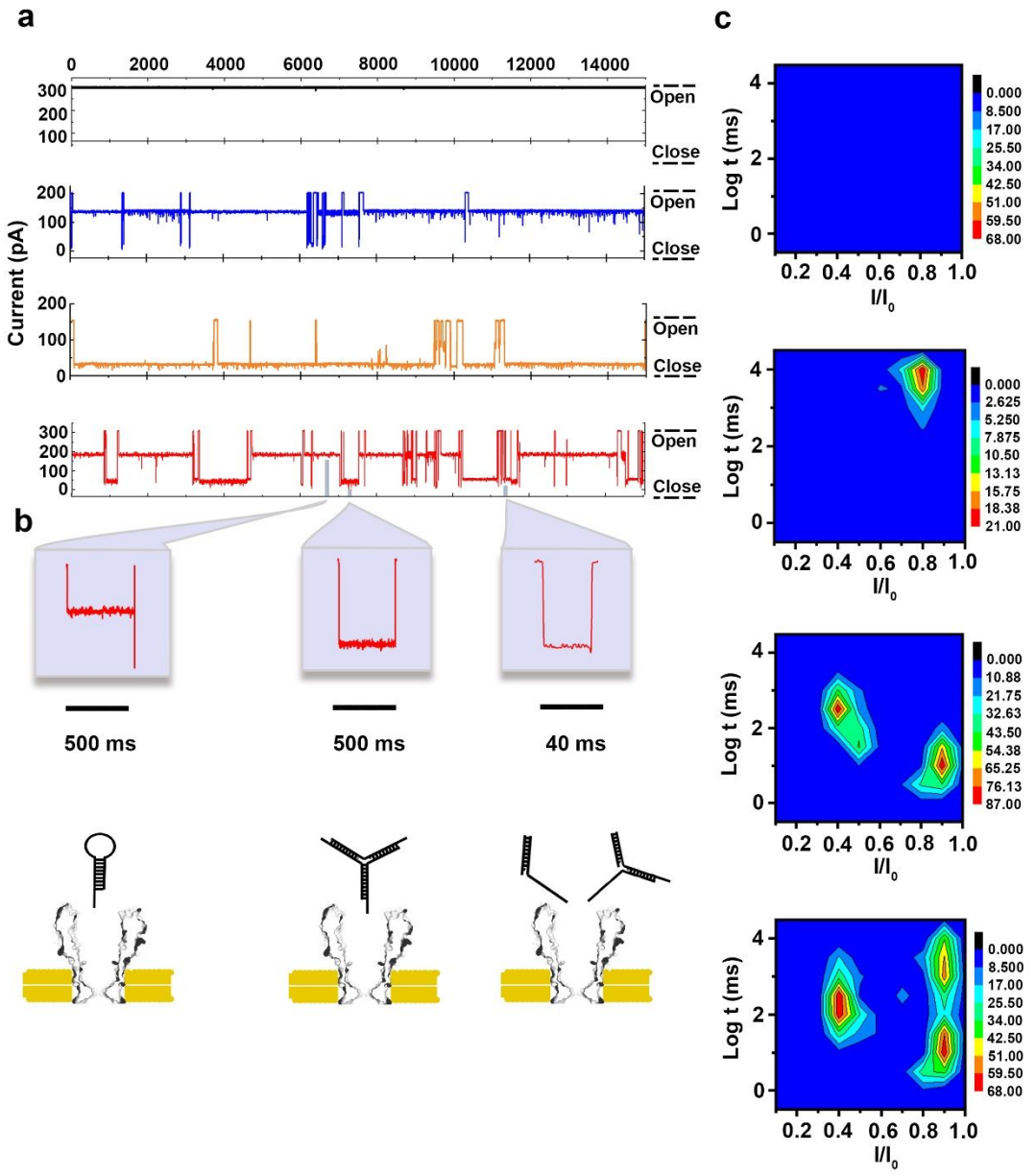


**Figure 2.** Characterization of hairpin and 3WJ structure using a MspA nanopore. (a) Representative current traces of the translocation of hairpin DNA (blue), 3WJ (orange) and P1+HA+HB+HC (red) through a MspA nanopore. The current trace in black shows the background of MspA nanopore. (b) Expanded view of three types of typical events, which associates with the translocation of hairpin and 3WJ through the nanopore, respectively. (c) 2D event-distribution plots, showing the signal distribution with nothing added, addition of hairpin, addition of 3WJ and addition of P1+HA+HB+HC. The distributions were plotted according to current blockade percentage and logarithm of dwell time. All data were obtained in the buffer of *cis*: 0.5 M NaCl, 10 mM Tris-HCl, pH 8.0, *trans*: 3 M NaCl, 10 mM Tris-HCl, pH 8.0 at a transmembrane potential of 100 mV.

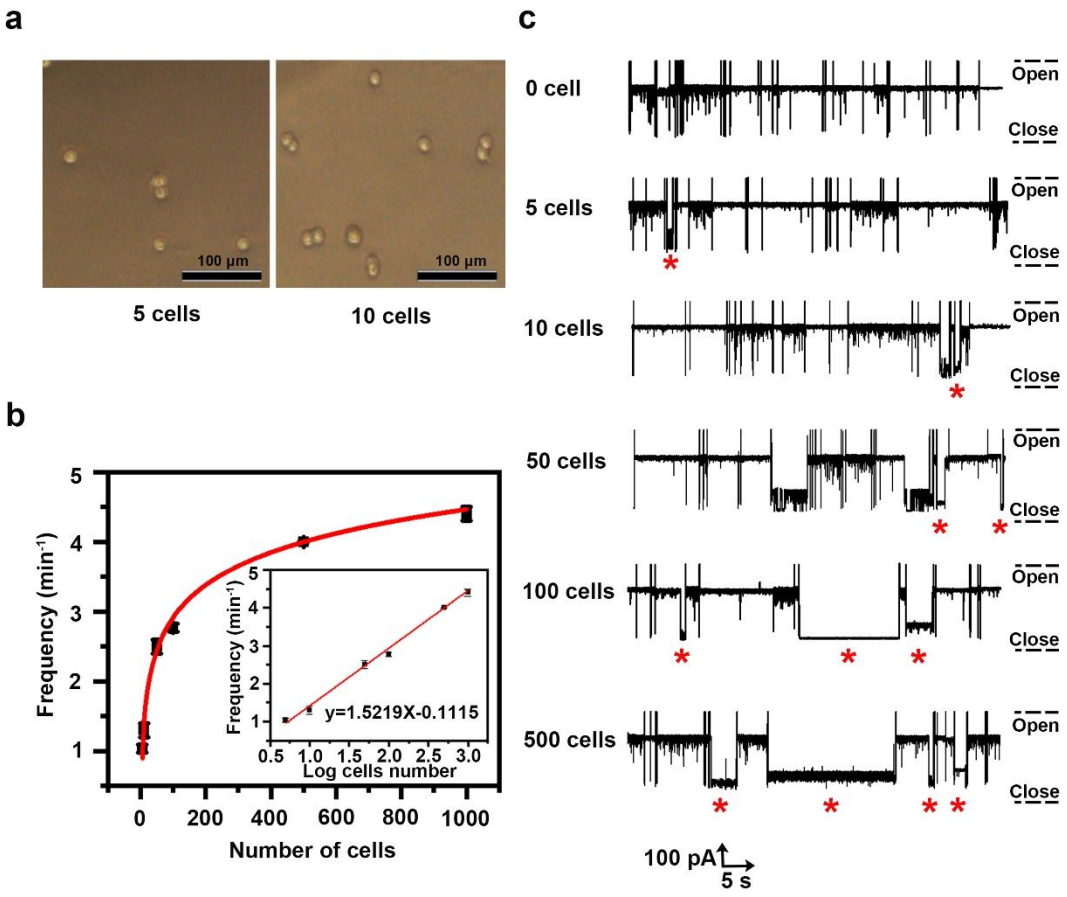


**Figure 3.** Quantitative limit of detection of breast cancer cell MCF-7. (a) Microscope images of 5 (left) and 10 (right) MCF-7 cells. (b) Correlation of the frequency of translocation events versus the number of cells ranging from 5 to 1000. The inset shows the linear relationship of event frequency and the logarithm of the number of cells (number of independent experiment n=3). (c) Current traces of the translocation of the 3WJ structure in the trigger of the number of MCF-7 cells (5, 10, 50, 100 and 500, respectively). Red star indicates the events generated by 3WJ translocation. All data were obtained in the buffer of *cis*: 0.5 M NaCl, 10 mM Tris-HCl, pH 8.0, *trans*: 3 M NaCl, 10 mM Tris-HCl, pH 8.0 at a transmembrane potential of 100 mV.

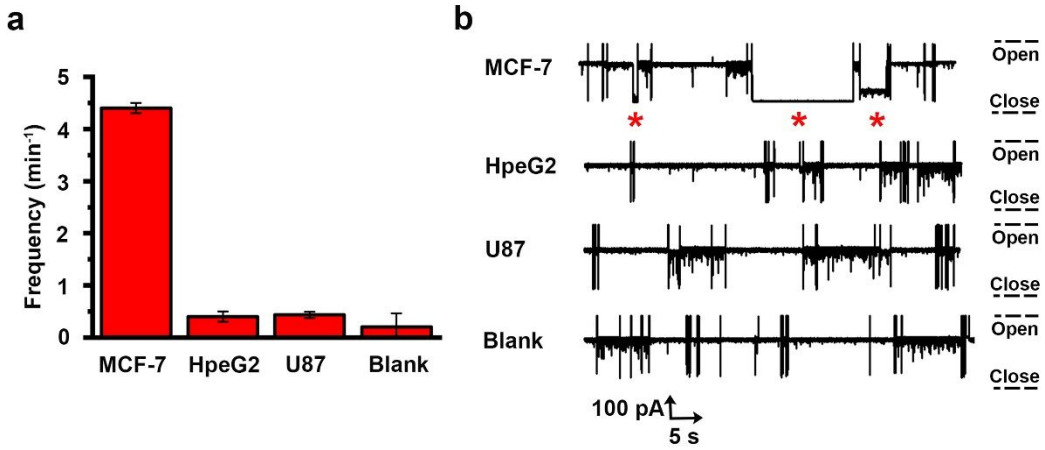


**Figure 4.** The specificity of nanopore assay for the detection of breast cancer cells. (a) The frequency of the translocation of 3WJ generated in response to MCF-7, HepG2 and U87 cells. (number of independent experiment n=3). (b) The representative current traces of the translocation of 3WJ structure generated in the trigger of MCF-7, HepG2 and U87 cells. The final number of these three types of cancer cell is 100. Red star indicated the events generated by 3WJ translocation. All data were obtained in the buffer of *cis*: 0.5 M NaCl, 10 mM Tris-HCl, pH 8.0, *trans*: 3 M NaCl, 10 mM Tris-HCl, pH 8.0 at a transmembrane potential of 100 mV.

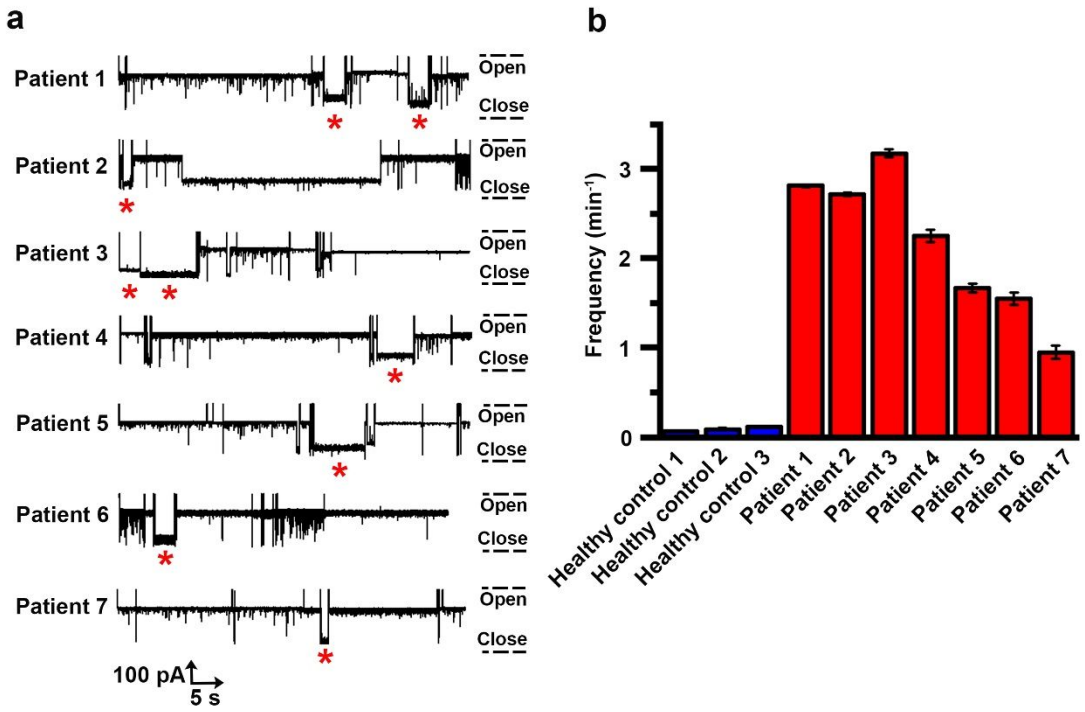


**Figure 5.** The detection CTCs in serum from healthy volunteers and breast cancer patients. (a) The representative current traces of the translocation of 3WJ structure generated in the trigger of CTCs cells in serum from seven breast cancer patients. Red star indicating the events generated by 3WJ translocation. (b) The detection of CTCs of three healthy volunteers (in blue) and seven breast cancer patients (in red) (number of independent experiment n=3). All data were obtained in the buffer of *cis*: 0.5 M NaCl, 10 mM Tris-HCl, pH 8.0, *trans*: 3 M NaCl, 10 mM Tris-HCl, pH 8.0 at a transmembrane potential of 100 mV.

**Table 1.** Recovery rate of CTCs by the nanopore assay (n=3).

| Add cells | Found cells | Recovery rate (%) |
|---|---|---|
| 0 | 0 | - |
| 10 | 9 ± 1 | 90 ± 0.1 |
| 100 | 103 ± 4 | 103 ± 0.4 |
| 250 | 214 ± 13 | 85.6 ± 0.5 |
| 500 | 476 ± 18 | 95.2 ± 0.4 |

**Table 2.** Nanopore detection of CTCs in clinical blood samples from breast cancer patients with TNM staging evaluation.

| Sample | Sample Volume (mL) | Number of CTCs | Concentration of CTCs (n/mL) | TNM staging |
|---|---|---|---|---|
| 1 | 4 | 83 | 21.25 | T3N3M0 ⅢC |
| 2 | 4 | 73 | 18.25 | T1N1M0 ⅡA |
| 3 | 6 | 135 | 22.50 | T2N1M0 ⅡB |
| 4 | 7 | 34 | 4.86 | T1N1M0 ⅡA |
| 5 | 7 | 16 | 2.29 | T2N2M0 ⅢA |
| 6 | 4 | 13 | 3.25 | T2N2M0 ⅢA |
| 7 | 4 | 5 | 1.25 | T2N3M0 ⅢC |

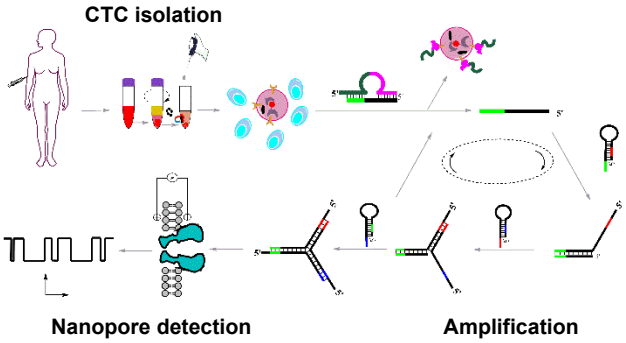


for TOC only